International Journal of Trend in Scientific Research and Development (IJTSRD)
Volume 10 Issue 2, Mar-Apr 2026 Available Online: www.ijtsrd.com e-ISSN: 2456 – 6470

The Chemistry Involved in the Birth and Death of Stars

Chijioke Onyia, Chukwujekwu N. Ofodum, Nnenna Ezenwukwa, Mercy Ezenwugo H., Monday Ugwuanyi, Nnamdi Ezeoyili M., Francis N. Obieti, Shaibu Abuh, Mercy Ogwu O., Peter Okagu, Obinna Okolo, Oluka Kwenyeluchi, Samuel Aneke, Lovelyn Nwagbo

Centre for Basic Space Science and Astronomy, Nsukka, Nigeria

ABSTRACT

Stars function as the universe's most efficient chemical reactors, driving the synthesis, transformation and redistribution of elements across cosmic time. This review examines the chemical processes underlying stellar birth, evolution and death, with emphasis on molecular, nuclear and isotopic pathways that govern elemental production. We begin with the astrochemistry of star-forming regions, highlighting gas-phase reactions, grain-surface chemistry and molecular complexity in collapsing molecular clouds. The sequential nuclear burning stages hydrogen, helium and advanced burning are discussed in terms of reaction networks, resonance phenomena and reaction-rate sensitivities that control elemental yields. Particular focus is placed on neutron-capture nucleosynthesis (s-, r- and p-processes), detailing their chemical signatures and dominant stellar environments. The chemical feedback from Asymptotic Giant Branch (AGB) stars, Supernovae and Neutron-star mergers is evaluated in the context of isotopic enrichment and elemental recycling into the interstellar medium. Again, unresolved chemical uncertainties, including key reaction rates and heavy-element production pathways are assessed. By integrating astrochemistry, nuclear chemistry and observational constraints, this review presents a coherent chemical framework for understanding the cosmic origin and evolutionary trend of the elements.

KEYWORDS: *Stellar nucleosynthesis; Astrochemistry; Nuclear burning; Neutron-capture processes (s-process, r-process, p-process); Asymptotic Giant Branch (AGB) stars; Supernovae; Neutron star mergers; Interstellar medium; Galactic chemical evolution; Molecular clouds.*

How to cite this paper: Chijioke Onyia | Chukwujekwu N. Ofodum | Nnenna Ezenwukwa | Mercy Ezenwugo H. | Monday Ugwuanyi | Nnamdi Ezeoyili M. | Francis N. Obieti | Shaibu Abuh | Mercy Ogwu O. | Peter Okagu | Obinna Okolo | Oluka Kwenyeluchi | Samuel Aneke | Lovelyn Nwagbo "The Chemistry Involved in the Birth and Death of Stars" Published in International Journal of Trend in Scientific Research and Development (ijtsrd), ISSN: 2456-6470, Volume-10 | Issue-2, April 2026, pp.654-667, URL: www.ijtsrd.com/papers/ijtsrd101393.pdf

IJTSRD101393

1. INTRODUCTION

The chemical complexity of the observable universe is one of the most profound consequences of stellar evolution. Every atom of carbon in organic molecules, every atom of oxygen in water, every atom of iron in haemoglobin and every atom of gold in terrestrial deposits was forged in the interior of a star or in the cataclysmic events surrounding stellar death [1]. As Carl Sagan famously noted, we are quite literally made of star-stuff. Understanding the precise chemical and nuclear processes by which stars create, redistribute and recycle the elements is therefore not merely an exercise in astrophysics; it is fundamental to understanding the chemical origins of planets, atmospheres, oceans and life itself [2].

The field of stellar nucleosynthesis was placed on firm theoretical footing by the seminal work of Burbidge, Burbidge, Fowler and Hoyle [1], commonly referred to as B^2FH and independently by Cameron [2]. These foundational papers outlined how the observed abundances of elements and isotopes in the solar system could be explained by a series of nuclear processes occurring in stars of different masses and at different evolutionary stages [3]. In the nearly seven decades, enormous progress has been made in nuclear physics experiments, computational stellar modelling, spectroscopic observations and most recently, multi-messenger astronomy, which have together refined and extended the original framework [4].

The chemistry of stellar birth begins long before nuclear fusion ignites in a protostellar core. Molecular clouds, the birthplaces of stars and rich in chemical species, including molecular hydrogen (H_2), carbon monoxide (CO), water (H_2O), ammonia (NH_3) and complex organic molecules such as amino acids and polycyclic aromatic hydrocarbons (PAHs) [5]. The chemical composition of these clouds, shaped by prior generations of stellar nucleosynthesis and the interstellar medium, determines the initial conditions for star formation and ultimately influences the types of planetary systems that may form around nascent stars [6].

This review aims to provide a comprehensive, up-to-date account of the chemistry involved at every stage of a star's life, from the initial chemical composition and molecular processes in star-forming regions, through the sequential nuclear burning stages that power stellar evolution, to the chemical enrichment of the interstellar medium by dying stars. We organize our discussion around the chronological narrative of a star's life, treating low-mass and high-mass evolutionary pathways in parallel where they diverge and we emphasize the chemical yields and nucleosynthetic products associated with each evolutionary phase.

Figure 1: Stellar Life Cycle — From Molecular Cloud to Stellar Remnant

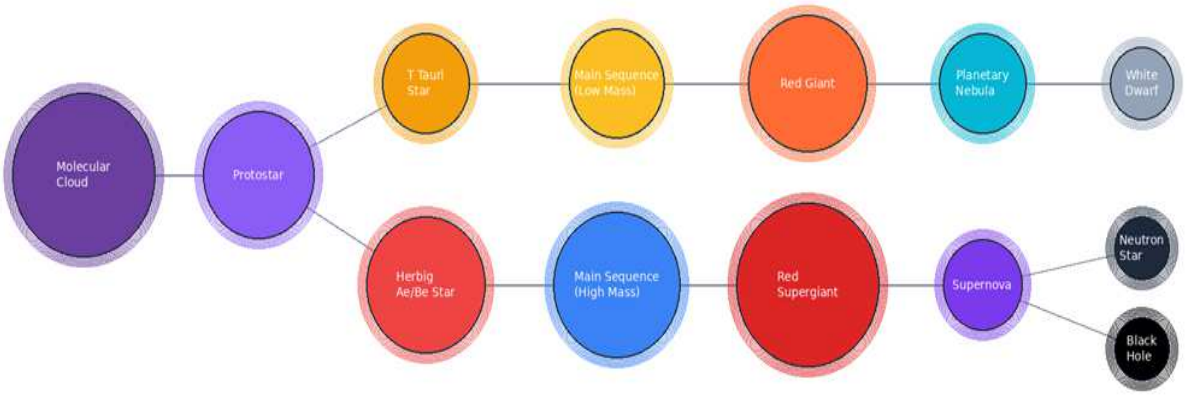

Low-mass path (M < 8 M☉): Cloud → Protostar → T Tauri → Main Seq → Red Giant → Planetary Nebula → White Dwarf

High-mass path (M ≥ 8 M☉): Cloud → Protostar → Herbig Ae/Be → Main Seq → Supergiant → Supernova → Neutron Star / Black Hole

Adapted from Iben (1967); Kippenhahn et al. (2012)

Figure 1. Schematic representation of the stellar life cycle, illustrating the divergent evolutionary pathways for low-mass ($M < 8\,M\odot$) and high-mass ($M \geq 8\,M\odot$) stars from molecular cloud to final stellar remnant. Adapted from [7] and [8]

1.1. Objectives of This Review

The principal objectives of this review article are as follows: Firstly, we seek to provide a thorough and accessible synthesis of the nuclear and chemical processes that govern each stage of stellar evolution, from molecular cloud chemistry and gravitational collapse through main-sequence hydrogen burning, post-main-sequence helium and advanced element burning, to the terminal phases of stellar death. Secondly, we aim to contextualize these processes within the broader framework of galactic chemical evolution, illustrating how successive generations of stellar birth and death progressively enrich the interstellar medium with heavier elements. Thirdly, we evaluate the current state of observational evidence, including stellar spectroscopy, isotopic measurements in meteoritic pre-solar grains, neutrino detections and gravitational-wave observations, that constrain theoretical models of nucleosynthesis. Fourthly, we identify and discuss the major open questions and frontiers in the field, including uncertainties in key nuclear reaction rates, the astrophysical site(s) of the r-process, the chemical yields of the first generation of stars and the role of binary stellar interactions in modifying nucleosynthetic outcomes. Finally, we highlight recent breakthroughs and future prospects, including the contributions of next-generation observatories, nuclear physics facilities and computational modelling to advancing our understanding of stellar chemistry.

2. Chemistry of Star-Forming Regions

2.1. Molecular Cloud Composition

Stars are born within giant molecular clouds (GMCs), vast structures of gas and dust with typical masses of 10^4 to 10^6 solar masses and temperatures of 10–20 K [9] Despite their name, molecular clouds are chemically diverse environments [10] The dominant molecular species is molecular hydrogen (H_2), which constitutes approximately 73% of the baryonic mass. The second most abundant molecule is carbon monoxide (CO), which serves as the primary observational tracer of molecular gas due to its readily detectable rotational emission lines at millimetre wavelengths [11]. Over 270 molecular species have been identified in the interstellar medium as of 2024, ranging from simple diatomics such as OH and CN to complex organic molecules including glycolaldehyde ($HCOCH_2OH$), acetamide (CH_3CONH_2) and even fullerenes (C_{60}) [6]

The chemical composition of a molecular cloud is not static but is continuously shaped by a complex interplay of gas-phase reactions, grain-surface chemistry, photo-dissociation, cosmic-ray ionization and thermal processes [12]. Ion-molecule reactions dominate the gas-phase chemistry at the low temperatures prevailing in cloud interiors, where neutral-neutral reactions with activation barriers are effectively suppressed. Cosmic rays, primarily high-energy protons, penetrate deep into cloud interiors and ionize H_2 to produce H_2^+, which then reacts with another H_2 to produce the crucial trihydrogen cation H_3^+. This ion drives a rich network of ion-molecule reactions that build up molecular complexity [13]

The key ionization reaction can be written as:

$$H_2 + \text{cosmic ray} \rightarrow H_2^+ + e^- \quad \text{Eq. (1)}$$

$$H_2^+ + H_2 \rightarrow H_3^+ + H \quad \text{Eq. (2)}$$

Grain-surface chemistry is equally important, particularly for the formation of H_2 itself, which cannot form efficiently in the gas phase under interstellar conditions. Hydrogen atoms adsorb onto the surfaces of interstellar dust grains, consisting primarily of silicates and carbonaceous material, where they diffuse and react to form H_2. More complex molecules, including water, methanol (CH_3OH) and formaldehyde (H_2CO) also formed via successive hydrogenation reactions on grain surfaces [14]; [15].

2.2. Gravitational Collapse and Protostellar Chemistry

When a region within a molecular cloud exceeds the Jeans mass, gravitational collapse is initiated. The Jeans mass, which represents the critical mass above which thermal pressure cannot support a cloud against its own gravity, is given by:

$$M_J = \left(\frac{5KT}{G\mu m_H}\right)^{3/2} \left(\frac{3}{4\pi\rho}\right)^{1/2} \quad \text{Eq. (3)}$$

where k is the Boltzmann constant, T is the temperature, G is the gravitational constant, μ is the mean molecular weight, m_H is the hydrogen atom mass and ρ is the density. For typical molecular cloud conditions ($T \approx 10$ K, $n \approx 10^4$ cm^{-3}), the Jeans mass is of the order of a few solar masses [16].

As collapse proceeds, the chemistry of the infalling material is significantly altered. Increasing densities cause molecular freeze-out onto grain surfaces, depleting the gas phase of species such as CO and N_2. In the inner regions, as temperature rises above ~100 K, ices sublimate releases complex molecules back into the gas phase in what is termed a hot corino (for low-mass protostars) or a hot core (for high-mass protostars) [17]. These warm, dense environments exhibit a particularly rich chemistry, with detections of numerous complex organic molecules including dimethyl ether, methyl formate and ethylene glycol [18].

The D/H (deuterium-to-hydrogen) ratio in molecules formed during this phase provides a powerful diagnostic of the physical conditions during star formation. Deuterium fractionation, driven by the exothermic exchange reaction $H_3^+ + HD \rightleftharpoons H_2D^+ + H_2$ at low temperatures, leads to dramatic enhancements of the D/H ratio above the cosmic value of $\sim 1.5 \times 10^{-5}$. Observations of multiply deuterated species such as D_2CO and ND_3 provide stringent constraints on the temperature and density history of protostellar material [17].

3. Main-Sequence Hydrogen Burning: The Chemistry of Stellar Energy Production

Once the core temperature of a contracting protostar reaches approximately 10^7 K, hydrogen fusion ignites and the star enters the main sequence, where it will spend the majority of its lifetime in hydrostatic equilibrium [19]. The conversion of hydrogen to helium is the defining chemical process of main-sequence stars, but the specific reaction pathway depends critically on the stellar mass and core temperature. Two principal mechanisms operate: the proton-proton (pp) chain and the carbon-nitrogen-oxygen (CNO) cycle [20].

3.1. The Proton-Proton Chain

The proton-proton chain is the dominant energy source in stars with masses below approximately 1.3 M⊙, including our Sun. It proceeds in three main branches (pp-I, pp-II and pp-III), with pp-I branch being the most probable under solar conditions. The pp-I chain consists of the following three reactions:

Step 1: $^{1}H + {}^{1}H \rightarrow {}^{2}H + e^{+} + ve$ (Q = 1.442 MeV) Eq. (4)

Step 2: $^{2}H + {}^{1}H \rightarrow {}^{3}He + \gamma$ (Q = 5.493 MeV) Eq. (5)

Step 3: $^{3}He + {}^{3}He \rightarrow {}^{4}He + 2{}^{1}H$ (Q = 12.860 MeV) Eq. (6)

The net effect is the conversion of four protons into one helium-4 nucleus, two positrons, two electron neutrinos and two gamma-ray photons, with a total energy release of 26.73 MeV [21]. The first step, the proton-proton fusion reaction, is the rate-limiting step because it requires the weak nuclear force to convert a proton into a neutron via positron emission [22]. The extremely low probability of this reaction (a mean reaction time of ~10^{9} years for any given proton pair) is what allows stars to burn hydrogen stably over billions of years rather than exploding [23].

Figure 3: The Proton-Proton Chain Reaction (pp-I Branch)

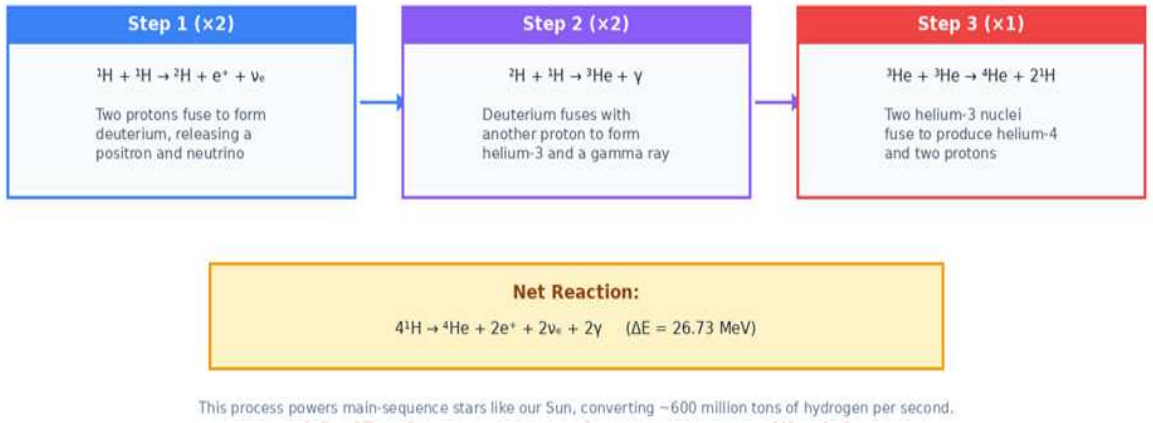

Figure 3. Schematic diagram of the proton-proton chain reaction (pp-I branch), showing the three sequential fusion steps and the net energy release. This process is the dominant energy source in solar-type stars.

The pp-II and pp-III branches become important at higher temperatures. In the pp-II branch, ^{3}He reacts with ^{4}He to produce ^{7}Be, which then captures an electron to form ^{7}Li, followed by proton capture and fission into two ^{4}He nuclei. The pp-III branch involves the decay of ^{8}B, producing high-energy neutrinos that are detectable on Earth and have been crucial for testing our understanding of solar physics [24].

3.2. The Carbon-Nitrogen-Oxygen (CNO) Cycle

In stars, more massive than approximately 1.3 M⊙, the CNO cycle becomes the dominant hydrogen-burning mechanism. First proposed by [19] and [20], the CNO cycle uses carbon, nitrogen and oxygen isotopes as catalysts in a cyclic series of proton captures and beta decays. The principal (CN) cycle consists of the following reactions:

$$^{12}C + {}^{1}H \rightarrow {}^{13}N + \gamma \quad \text{Eq. (7)}$$

$$^{13}N \rightarrow {}^{13}C + e^{+} + ve \quad \text{Eq. (8)}$$

$$^{13}C + {}^{1}H \rightarrow {}^{14}N + \gamma \quad \text{Eq. (9)}$$

$$^{14}N + {}^{1}H \rightarrow {}^{15}O + \gamma \quad \text{Eq. (10)}$$

$$^{15}O \rightarrow {}^{15}N + e^{+} + ve \quad \text{Eq. (11)}$$

$$^{15}N + {}^{1}H \rightarrow {}^{12}C + {}^{4}He \quad \text{Eq. (12)}$$

Fig 4: The Carbon-Nitrogen-Oxygen (CNO) Cycle

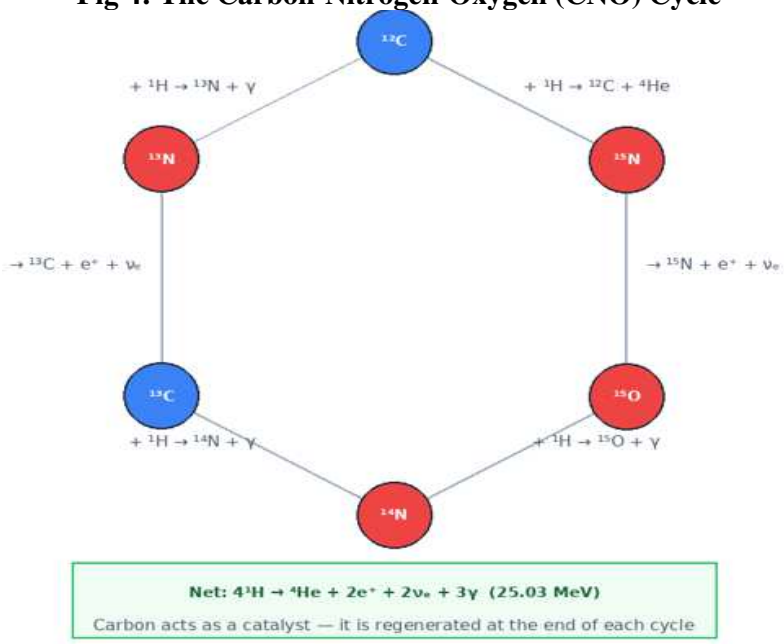

Figure 4. The Carbon-Nitrogen-Oxygen (CNO) cycle. Carbon-12 acts as a catalyst and is regenerated at the end of each cycle. The net result is identical to the pp-chain: four protons are converted into one helium-4 nucleus.

The net reaction is identical to the pp-chain: four protons are converted into one helium-4 nucleus with a total energy release of 25.03 MeV (slightly less than the pp-chain due to higher-energy neutrino losses) [25]. A critical feature of the CNO cycle is its extreme temperature sensitivity: the energy generation rate scales approximately as T^{16}, compared to T^4 for the pp-chain. This steep temperature dependence means that the CNO cycle produces a highly concentrated energy flux in stellar cores, driving convective energy transport in massive main-sequence stars [8].

An important chemical consequence of CNO-cycle operation is the conversion of most of the initial carbon and oxygen into nitrogen-14 at equilibrium, since the $^{14}N(p,\gamma)^{15}O$ reaction is the slowest step in the cycle. This explains the observed nitrogen enrichment in the atmospheres of massive stars and in the ejecta of stellar winds and supernovae [26]; [27].

Figure 2: Hertzsprung-Russell Diagram

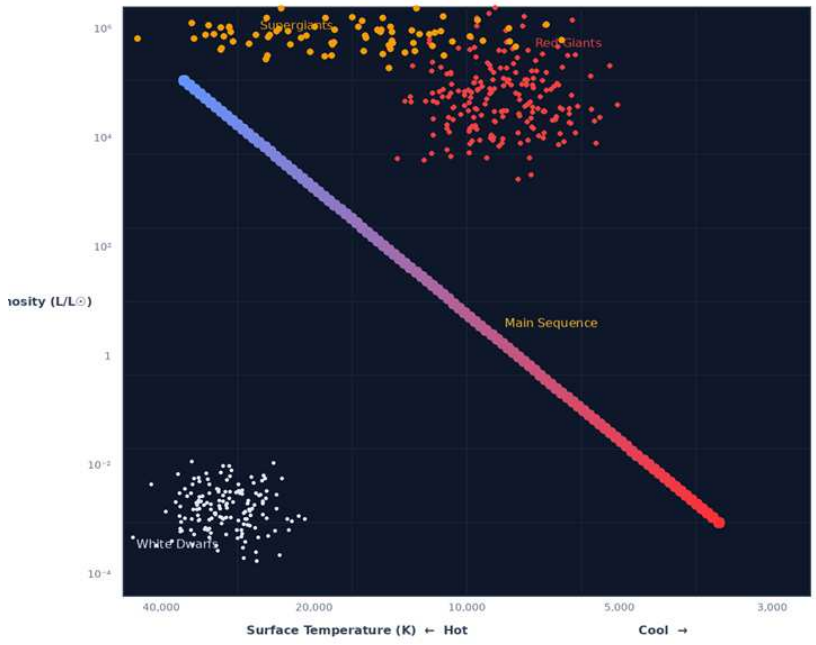

Figure 2. The Hertzsprung-Russell diagram showing the principal stellar populations: main sequence, red giants, supergiants and white dwarfs. The position of a star on this diagram is determined by its surface temperature and luminosity, which in turn reflect its internal chemical and nuclear processes. [28]

4. Helium Burning and the Triple-Alpha Process

Following the exhaustion of hydrogen in the core, stars evolve off the main sequence. For stars of all masses, the next major nucleosynthetic phase is helium burning, which becomes possible when core temperatures reach approximately 10^8 K. The fusion of helium into carbon proceeds via the celebrated triple-alpha (ααα or 3α) process, first explained by [29] Salpeter (1952) and [30].

The triple-alpha process occurs in two steps. First, two helium-4 nuclei (alpha particles) combine to form beryllium-8, which is highly unstable with a lifetime of only ~10^{-16} seconds:

$$^4\text{He} + ^4\text{He} \rightleftharpoons ^8\text{Be} \ (\Delta t \approx 10^{-16} \text{ s}) \text{ Eq. (13)}$$

Before the ^{8}Be can decay, a third alpha particle must be captured to form carbon-12. This reaction is possible only because of a remarkable coincidence: the existence of an excited nuclear state of ^{12}C at 7.654 MeV, known as the Hoyle state, which acts as a resonance that dramatically enhances the reaction rate:

$$^8\text{Be} + ^4\text{He} \rightarrow ^{12}\text{C}^* \rightarrow ^{12}\text{C} + \gamma \ (Q = 7.275 \text{ MeV}) \text{ Eq. (14)}$$

The existence of this resonance was predicted by [30] on purely astrophysical grounds, namely, the requirement that carbon be produced in sufficient quantities to explain its observed cosmic abundance, before it was experimentally confirmed by [31]. This prediction is often cited as one of the most remarkable examples of anthropic reasoning in physics [32]. The combined net reaction of the triple-alpha process is:

$$3\ ^4\text{He} \rightarrow ^{12}\text{C} + \gamma \ (Q = 7.275 \text{ MeV}) \text{ Eq. (15)}$$

Once a sufficient abundance of ^{12}C has been built up, a competing reaction becomes important: the capture of an additional alpha particle by ^{12}C to produce oxygen-16:

$$^{12}\text{C} + ^4\text{He} \rightarrow ^{16}\text{O} + \gamma \ (Q = 7.162 \text{ MeV}) \text{ Eq. (16)}$$

The ratio of the ^{12}C(α,γ)^{16}O reaction rate to the triple-alpha rate is one of the most critically important quantities in all of nuclear astrophysics. It determines the C/O ratio at the end of helium burning, which in turn profoundly influences all subsequent nucleosynthetic stages, the properties of white dwarfs, the outcomes of Type Ia supernovae and ultimately, the abundances of carbon and oxygen in the universe. Despite decades of experimental and theoretical effort, this rate remains uncertain at the ~20–30% level, representing one of the key unresolved problems in nuclear astrophysics [33].

In low-mass stars ($M < 8\ M_\odot$), helium burning occurs in the degenerate core during the helium flash (for $M < 2.3\ M_\odot$) or quiescently in more massive intermediate-mass stars. The products of helium burning, primarily carbon and oxygen, form the composition of the resulting white dwarf. In massive stars, helium burning occurs stably in the core and produces a carbon-oxygen core that will undergo further nuclear processing [12].

5. Advanced Nuclear Burning Stages in Massive Stars

Stars with initial masses exceeding approximately 8 $M_\odot$ achieve core temperatures sufficient to ignite a series of progressively heavier nuclear fuels following helium exhaustion [34]. These advanced burning stages proceed with dramatically accelerating timescales due to the increasing importance of neutrino energy losses, which carry energy directly out of the star far more efficiently than photon radiation from the surface [35]. This sequence of burning stages creates a characteristic onion-shell structure in the stellar interior, with each concentric shell burning a successively lighter fuel [4].

Figure 5: Onion-Shell Structure of a Massive Star Before Core Collapse

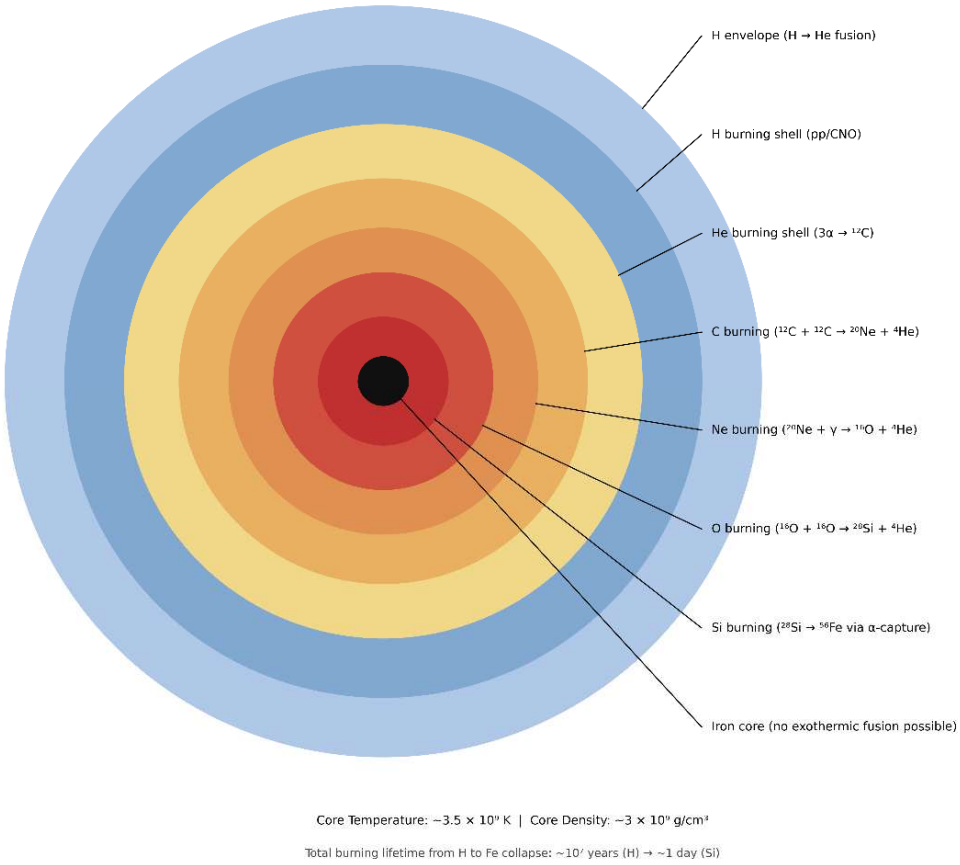

Figure 5. The onion-shell structure of a massive star ($M \geq 8\ M\odot$) just prior to core collapse, showing the concentric layers of nuclear burning. Each shell processes a different nuclear fuel, with an inert iron core at the center. The burning timescales decrease dramatically inward, from millions of years for hydrogen to approximately one day for silicon.

5.1. Carbon Burning

Carbon burning ignites at core temperatures of approximately 6×10^8 K and densities of ~2×10^5 g cm^{-3}. The principal reaction involves the fusion of two carbon-12 nuclei, which produces a compound nucleus of ^{24}Mg* that promptly decays through several channels:

$$^{12}C + {}^{12}C \rightarrow {}^{24}Mg^* \rightarrow {}^{20}Ne + {}^{4}He \ (Q = 4.617\ MeV) \quad \text{Eq. (17)}$$

$$^{12}C + {}^{12}C \rightarrow {}^{23}Na + {}^{1}H \ (Q = 2.241\ MeV) \quad \text{Eq. (18)}$$

$$^{12}C + {}^{12}C \rightarrow {}^{23}Mg + n \ (Q = -2.599\ MeV) \quad \text{Eq. (19)}$$

The alpha particles, protons and neutrons released in these reactions participate in secondary reactions that produce a range of isotopes including ^{16}O, ^{20}Ne, ^{23}Na, ^{24}Mg, ^{25}Mg and ^{26}Mg. Carbon burning in a 25 M⊙ star lasts approximately 600 years [34].

5.2. Neon Burning

At temperatures exceeding ~1.2×10^9 K, neon burning commences. Unlike the previous burning stages, neon burning is initiated by photodisintegration rather than fusion. High-energy gamma rays break apart ^{20}Ne nuclei in a process that is endothermic but is thermodynamically favoured at these extreme temperatures:

$$^{20}Ne + \gamma \rightarrow {}^{16}O + {}^{4}He \ (Q = -4.730\ MeV) \quad \text{Eq. (20)}$$

The liberated alpha particles are then captured by remaining ^{20}Ne nuclei in a strongly exothermic reaction:

$$^{20}Ne + {}^{4}He \rightarrow {}^{24}Mg + \gamma \ (Q = 9.316\ MeV) \quad \text{Eq. (21)}$$

The net effect of neon burning is therefore the conversion of two neon-20 nuclei into one oxygen-16 and one magnesium-24, with a net positive energy release. This stage lasts only about one year in a 25 M⊙ star [36].

5.3. Oxygen Burning

Oxygen burning ignites at temperatures of ~2×10^9 K and proceeds via the fusion of two oxygen-16 nuclei:

$$^{16}O + {}^{16}O \rightarrow {}^{28}Si + {}^{4}He \ (Q = 9.594 \text{ MeV}) \quad \text{Eq. (22)}$$

$$^{16}O + {}^{16}O \rightarrow {}^{31}P + {}^{1}H \ (Q = 7.678 \text{ MeV}) \quad \text{Eq. (23)}$$

$$^{16}O + {}^{16}O \rightarrow {}^{31}S + n \ (Q = 1.500 \text{ MeV}) \quad \text{Eq. (24)}$$

The principal products are silicon-28, sulfur-32, argon, calcium and various intermediate-mass elements. Oxygen burning lasts approximately six months in a 25 M⊙ star [34].

5.4. Silicon Burning and Nuclear Statistical Equilibrium

The final major burning stage, silicon burning occurs at temperatures exceeding 3×10^9 K. At these extreme temperatures, photo-disintegration becomes ubiquitous. Silicon-28 nuclei are partially photo-disintegrated, releasing alpha particles, protons and neutrons that are rapidly recaptured by other nuclei in a complex network of thousands of reactions. Rather than proceeding by a single well-defined fusion reaction, silicon burning is better described as a quasi-equilibrium process in which nuclear reactions proceed in both directions at comparable rates, driving the composition toward nuclear statistical equilibrium (NSE).

The composition at NSE is determined by the temperature, density and neutron-to-proton ratio (or equivalently, the electron fraction Y_e). Under the conditions prevailing in massive stellar cores ($Y_e \approx 0.42$–0.44), NSE strongly favours nuclei in the iron-peak region, particularly ^{56}Ni, ^{56}Fe, ^{54}Fe, ^{58}Ni and ^{52}Cr. Silicon burning lasts only about one day, after which the star has an inert iron core that cannot release energy through further fusion, setting the stage for core collapse [37]; [34].

Table 1: Timescales of Nuclear Burning Stages in a 25 M⊙ Star

Burning Stage	Primary Fuel	T (K)	Products	Duration
Hydrogen	H (pp/CNO)	~4×10^7	He	~7×10^6 yr
Helium	He (3α)	~2×10^8	C, O	~5×10^5 yr
Carbon	$^{12}C + {}^{12}C$	~6×10^8	Ne, Na, Mg	~600 yr
Neon	$^{20}Ne + \gamma$	~1.2×10^9	O, Mg	~1 yr
Oxygen	$^{16}O + {}^{16}O$	~2×10^9	Si, S	~6 months
Silicon	Si (α-captures)	~3.5×10^9	Fe, Ni	~1 day

Table 1. Sequential nuclear burning stages in a 25 M⊙ star, showing the characteristic temperatures, products and dramatically decreasing timescales. Data from [34] and [4].

6. Neutron-Capture Nucleosynthesis: Building Elements Beyond Iron

The synthesis of elements heavier than iron ($Z > 26$) cannot proceed by charged-particle fusion reactions under stellar conditions because the Coulomb barrier becomes prohibitively large and the binding energy per nucleon decreases beyond the iron peak [38]. Instead, the trans-iron elements are primarily produced by neutron-capture processes, in which seed nuclei (typically iron-peak elements) capture neutrons one at a time, building up heavier isotopes. Two distinct neutron-capture processes operate, distinguished by the timescale of neutron capture relative to beta decay: the slow process (s-process) and the rapid process (r-process) [1]; [39].

6.1. The Slow Neutron-Capture Process (s-process)

The s-process occurs under conditions of relatively low neutron density ($n_n \approx 10^6$–10^{11} cm^{-3}), such that the timescale for neutron capture is much longer than the timescale for beta decay for most unstable nuclei along the neutron-capture path [18]. The s-process therefore follows the valley of beta stability closely, building up nuclei by successive neutron captures with occasional beta decays when an unstable isotope is produced. The generic s-process reaction can be written as:

$$(Z, A) + n \rightarrow (Z, A+1) + \gamma \quad \text{Eq. (25)}$$

$$\text{If } (Z, A+1) \text{ is unstable: } (Z, A+1) \rightarrow (Z+1, A+1) + e^- + \nu e \quad \text{Eq. (26)}$$

The main site of the s-process is the thermally pulsing asymptotic giant branch (TP-AGB) phase of low- and intermediate-mass stars (1–8 M⊙). Two principal neutron sources operate in AGB stars. The $^{13}C(\alpha,n)^{16}O$ reaction operates during the interpulse phase in a thin ^{13}C pocket, providing most of the neutron exposure, while the $^{22}Ne(\alpha,n)^{25}Mg$ reaction operates at higher temperatures during thermal pulses and is especially important in more massive AGB stars [35]; [3].

The s-process produces approximately half of the isotopes heavier than iron, including important contributions to strontium, barium, lanthanum, cerium and lead. The s-process abundance pattern shows characteristic peaks at neutron magic numbers (N = 50, 82, 126), corresponding to nuclei with closed neutron shells that have particularly low neutron-capture cross sections: ^{88}Sr, ^{138}Ba and ^{208}Pb [39].

6.2. The Rapid Neutron-Capture Process (r-process)

The r-process requires extremely high neutron densities ($n_n > 10^{20}$ cm^{-3}) and short timescales (seconds), conditions under which neutron capture is far faster than beta decay. The capture path therefore runs far from stability on the neutron-rich side of the nuclear chart, building up extremely neutron-rich isotopes that subsequently beta-decay back toward stability once the neutron flux subsides. The r-process produces approximately half of the isotopes heavier than iron, as well as all of the naturally occurring actinides (thorium, uranium) and is the dominant source of elements such as europium, platinum, gold and iridium [40]; [41].

The astrophysical site(s) of the r-process has been one of the longest-standing open questions in nuclear astrophysics. Core-collapse supernovae were long considered the primary candidate, but modern simulations have had difficulty producing the required conditions in the neutrino-driven wind [21]. A landmark observation came on August 17, 2017, when the LIGO-Virgo gravitational-wave detectors observed the neutron star merger event GW170817, accompanied by an electromagnetic counterpart (kilonova) whose light curve and spectra provided strong evidence for copious r-process nucleosynthesis, including the production of lanthanides and possibly actinides ([42]; [31]; [43]). Current evidence suggests that neutron star mergers are a major and possibly the dominant source of r-process elements, though contributions from rare types of core-collapse supernovae (such as magneto-rotational supernovae and collapsars) may also be significant ([44]; [40]).

6.3. The p-Process and Other Proton-Rich Nucleosynthesis

A small fraction of stable isotopes on the proton-rich side of the valley of stability cannot be produced by either the s- or r-processes. These so-called p-nuclei (approximately 35 isotopes, including ^{92}Mo, ^{96}Ru and ^{196}Hg) are produced by a combination of photo-disintegration reactions (the γ-process) in the oxygen-neon-rich layers of core-collapse supernovae and possibly by the νp-process in neutrino-driven winds ([45]; [41]). The p-process remains one of the least well-understood areas of nucleosynthesis, with current models unable to simultaneously reproduce the abundances of all p-nuclei.

Figure 6: Origin of Elements — Nucleosynthetic Processes

Figure 6. The origin of elements by nucleosynthetic process. Different colours indicate the dominant production mechanism for each element, from Big Bang nucleosynthesis (lightest elements) through stellar fusion, s-process, r-process and other channels. [32] and [46].

7. Chemical Consequences of Stellar Death

The manner in which a star ends its life determines the quantity, composition and distribution of the chemically enriched material it returns to the interstellar medium. The dominant modes of stellar death span a remarkable range of phenomena, from the gentle mass loss of AGB stellar winds to the most energetic explosions in the universe.

7.1. Low- and Intermediate-Mass Stars: AGB Winds and Planetary Nebulae

Stars with initial masses in the range 1–8 M⊙ do not undergo core collapse. Instead, they lose their outer envelopes through powerful stellar winds during the AGB phase, exposing the hot carbon-oxygen core that becomes a white dwarf. The ejected material forms a planetary nebula, a shell of ionized gas enriched in

the products of hydrogen and helium shell burning [3]. The chemical yields of AGB stars include substantial amounts of helium, carbon-12 (from the triple-alpha process, dredged to the surface by convective mixing episodes known as third dredge-up), nitrogen-14 (from CNO processes, especially via hot-bottom burning in more massive AGB stars) and s-process elements. AGB stars are the dominant source of carbon, fluorine and s-process elements such as barium and lead in the Galaxy [47].

7.2. Core-Collapse Supernovae

Stars with initial masses exceeding ~8 M⊙ end their lives in core-collapse supernovae (Types II, Ib, Ic), releasing approximately 3×10^{53} erg of gravitational binding energy, of which ~99% is carried away by neutrinos and ~1% (approximately 10^{51} erg, or 1 foe) is deposited in the kinetic energy of the ejecta [4]. The nucleosynthetic products depend on the progenitor mass, metallicity, explosion energy and the mass cut (the boundary between material that falls onto the remnant and material that is ejected). Core-collapse supernovae are the dominant producers of elements from oxygen through the iron peak, including oxygen, neon, magnesium, silicon, sulphur, argon, calcium, titanium, chromium, manganese, iron, cobalt and nickel [48].

A particularly important radio-isotope produced in core-collapse supernovae is ^{56}Ni, which decays through ^{56}Co to stable ^{56}Fe with a combined half-life of ~111 days. The energy released by this radioactive decay chain powers the light curve of the supernova from weeks to months after the explosion. The amount of ^{56}Ni synthesized, typically 0.01–0.3 M⊙ for core-collapse events, is a key diagnostic of the explosion physics ([36]; [49]).

7.3. Type Ia Supernovae

Type Ia supernovae are thermonuclear explosions of carbon-oxygen white dwarfs in binary systems. The standard model involves a white dwarf accreting matter from a companion star until it approaches the Chandrasekhar mass limit (~1.4 M⊙), at which point compressional heating ignites a thermonuclear runaway that unbinds the entire star [50]. The explosion synthesizes approximately 0.5–0.8 M⊙ of ^{56}Ni (which decays to ^{56}Fe), along with significant quantities of silicon, sulphur, calcium and other intermediate-mass elements. Type Ia supernovae are the dominant source of iron-peak elements in the universe and play a crucial role as cosmological distance indicators due to the standardizable nature of their peak luminosities [51].

7.4. Neutron Star Mergers and Kilonovae

The coalescence of two neutron stars or a neutron star with a black hole, ejects highly neutron-rich material that undergoes vigorous r-process nucleosynthesis. The radioactive decay of the freshly synthesized r-process elements powers a thermal transient known as a kilonova (or macronova). The detection and spectroscopic analysis of the kilonova AT2017gfo, associated with the gravitational-wave event GW170817 provided the first direct observational confirmation of r-process nucleosynthesis in a neutron star merger. The identification of spectral features attributed to strontium [52] and the inference of lanthanide-rich ejecta from the red kilonova component [53] have transformed our understanding of the origin of the heaviest elements. Current estimates suggest that a single neutron star merger can produce ~0.01–0.05 M⊙ of r-process material, including elements such as gold, platinum and uranium ([54]; [40]).

8. Galactic Chemical Evolution (GCE)

The chemical evolution of a galaxy describes the time-dependent build-up of elemental abundances in its interstellar medium and stars as successive generations of stars form, evolve and die [55]. The framework of Galactic Chemical Evolution (GCE) integrates stellar nucleosynthetic yields with models of star formation, gas inflows and outflows and stellar dynamics to predict the distribution of elemental abundances observed in stars of different ages and locations within a galaxy [32].

A key observational diagnostic in GCE is the ratio of alpha-elements (O, Ne, Mg, Si, S, Ca, Ti) to iron. Core-collapse supernovae, which occur promptly (~10^6–10^7 years after star formation) produce large amounts of alpha-elements relative to iron [56]. Type Ia supernovae which have longer delay times (~10^8–10^9 years due to the need for a white dwarf to accrete to the Chandrasekhar limit) and the dominant producers of iron-peak elements. This difference in timescales creates a characteristic "knee" in the [α/Fe] vs. [Fe/H] diagram: at low metallicities, [α/Fe] is enhanced (~+0.4 dex) due to the exclusive contribution of core-collapse supernovae, while at higher metallicities, [α/Fe] decreases as Type Ia supernovae begin to contribute their iron [57] [13]).

The chemical abundances observed in Extremely Metal-Poor (EMP) stars, with [Fe/H] < −3, provide crucial constraints on the nucleosynthetic yields of the first stellar generations. Some EMP stars show dramatic enhancements of carbon (the carbon-enhanced metal-poor, or CEMP, stars), while others show r-process enhancement (the so-called r-II stars such as CS 22892-052 and J0954+5246). These abundance patterns offer windows into the chemical yields of the earliest supernovae and possibly of Population III stars [58]; [59].

Recent advances in GCE modelling have incorporated the contributions of neutron star mergers to r-process enrichment, accounting for the delay-time distribution of compact binary mergers. Additionally, high-resolution spectroscopic surveys such as APOGEE, GALAH and Gaia-ESO have provided chemical abundances for millions of stars across the Milky Way, enabling "chemical cartography" of the Galaxy and revealing the complex interplay between chemical enrichment, stellar migration and dynamical evolution ([60]; [61]).

9. Open Questions and Future Directions

Despite enormous progress, several fundamental questions in stellar chemistry remain open. We highlight the most significant current challenges and the observational and experimental efforts that are expected to address them in the coming decade.

9.1. The $^{12}C(\alpha,\gamma)^{16}O$ Reaction Rate

As discussed in Section 4, the rate of alpha capture on carbon-12 at helium-burning temperatures remains uncertain by ~20–30%, representing one of the most consequential unsolved problems in nuclear astrophysics. New experimental programs at underground nuclear physics laboratories (e.g., LUNA, CASPAR, JUNA) and advances in ab initio nuclear theory are expected to reduce this uncertainty significantly over the next decade [33].

9.2. The Astrophysical Site(s) of the r-Process

While the GW170817 observation established neutron star mergers as a confirmed r-process site, questions remain about whether they are the sole or even dominant site. The observed r-process enrichment in some ultra-faint dwarf galaxies and in certain early-universe stars is difficult to reconcile with the expected merger delay times and event rates [62]. Alternative or additional sites, including magneto-rotational supernovae, collapsars and common-envelope jet supernovae are actively being investigated through both theoretical simulations and observational surveys [44]; [63].

9.3. Population III Stars and Early Enrichment

The first stars to form in the universe (Population III) were composed entirely of hydrogen and helium produced in Big Bang nucleosynthesis. Their nucleosynthetic yields, mass function and explosion properties remain poorly constrained by observations, though indirect evidence comes from the abundance patterns of EMP stars [10]. The James Webb Space Telescope (JWST) may detect signatures of Population III stars or their supernovae at high redshift, while next-generation spectroscopic surveys will continue to discover and analyze EMP stars in the Milky Way halo [25].

10. Conclusions

Stars are the universe's pre-eminent chemical laboratories responsible for transforming the primordial hydrogen and helium produced in the Big Bang into the rich array of elements that compose the planets, oceans, atmospheres and living organisms. This review has traced the complete chemical narrative of stellar evolution, from the complex molecular chemistry of star-forming clouds, through the precisely ordered sequence of nuclear burning stages that power stellar lifetimes, to the dramatic chemical enrichment events that accompany stellar death.

The principal nuclear reaction sequences, including the proton-proton chain, the CNO cycle, the triple-alpha process and the advanced burning stages of carbon, neon, oxygen and silicon, represent a grand chemical cascade in which each stage creates the fuel for the next, culminating in the production of iron-peak elements at the endpoint of exothermic fusion. Beyond iron, the slow and rapid neutron-capture processes extend the reach of nucleosynthesis across the entire periodic table, with the s-process operating in the quiescent interiors of AGB stars and the r-process occurring in the most extreme environments in the universe: neutron star mergers and possibly certain classes of supernovae.

The observational landscape has been transformed in recent years by multi-messenger astronomy, with the landmark detection of gravitational waves from the neutron star merger GW170817 and its associated kilonova providing direct evidence for r-process nucleosynthesis. Large-scale spectroscopic surveys have mapped the chemical abundances of millions of stars across the Milky Way, revealing the complex history of galactic chemical evolution. Meanwhile, advances in nuclear physics experiments, computational astrophysics space and ground-based observatories continue to refine our understanding of the nuclear reaction rates, stellar models and enrichment timescales that govern the chemical evolution of the cosmos.

As we look to the future, the convergence of next-generation gravitational-wave detectors, neutrino observatories, radioactive-ion-beam facilities, spectroscopic surveys and the James Webb Space Telescope promises to address many of the remaining open questions in stellar nucleosynthesis and usher in a new era of precision stellar chemistry. The ancient question of the origin of the elements is now answered in broad outlines, but its full resolution, down to the last isotopic detail remains one of the grand challenges of modern astrophysics.

References

[1] Burbidge, E. M., Burbidge, G. R., Fowler, W. A., & Hoyle, F. (1957). Synthesis of the elements in stars. *Reviews of modern physics*, *29*(4), 547.

[2] Cameron, A. G. W. (1957). Nuclear reactions in stars and nucleogenesis. *Publications of the Astronomical Society of the Pacific*, *69*(408), 201-222.

[3] Karakas, A. I., & Lattanzio, J. C. (2014). The Dawes review 2: nucleosynthesis and stellar yields of low-and intermediate-mass single stars. *Publications of the Astronomical Society of Australia*, *31*, e030.

[4] Nomoto, K. I., Kobayashi, C., & Tominaga, N. (2013). Nucleosynthesis in stars and the chemical enrichment of galaxies. *Annual Review of Astronomy and Astrophysics*, *51*, 457-509.

[5] Herbst, E., & van Dishoeck, E. F. (2009). Complex organic interstellar molecules. *Annual Review of Astronomy and Astrophysics,* 47, 427–480.

[6] Tielens, A. G. G. M. (2013). The molecular universe. *Reviews of Modern Physics*, *85*(3), 1021-1081.

[7] Iben Jr, I. (1967). Stellar evolution within and off the main sequence. *Annual Review of Astronomy and Astrophysics, vol. 5, p. 571*, *5*, 571.

[8] Kippenhahn, R., Weigert, A., & Weiss, A. (2012). Stellar Structure and Evolution (2nd ed.). Springer-Verlag.

[9] Horowitz, C. J., Arcones, A., Cote, B., Dillmann, I., Nazarewicz, W., Roederer, I. U., ... & Wang, M. (2019). r-process nucleosynthesis: connecting rare-isotope beam facilities with the cosmos. *Journal of Physics G: Nuclear and Particle Physics*, *46*(8), 083001.

[10] Bromm, V. (2013). Formation of the first stars. *Reports on Progress in Physics*, *76*(11), 112901.

[11] McGuire, B. A. (2022). 2021 census of interstellar, circumstellar, extragalactic, protoplanetary disk and exoplanetary molecules. *The Astrophysical Journal Supplement Series*, *259*(2), 30.

[12] Herbst, E., & Klemperer, W. (1973). The formation and depletion of molecules in dense interstellar clouds. The Astrophysical Journal, 185, 505–533.

[13] McWilliam, A. (1997). Abundance ratios and galactic chemical evolution. *Annual Review of Astronomy and Astrophysics*, *35*(1), 503-556.

[14] Watanabe, N., & Kouchi, A. (2002). Efficient formation of formaldehyde and methanol by the addition of hydrogen atoms to CO in H2O-CO ice at 10 K. *The Astrophysical Journal Letters*, *571*(2), L173-L176.

[15] Cuppen, H. M., Walsh, C., Lamberts, T., Semenov, D., Garrod, R. T., Penteado, E. M., & Ioppolo, S. (2017). Grain surface models and data for astrochemistry. *Space Science Reviews*, *212*(1), 1-58.

[16] Stahler, S. W., & Palla, F. (2008). *The formation of stars*. John Wiley & Sons.

[17] Ceccarelli, C., Dominik, C., López-Sepulcre, A., Kama, M., Padovani, M., Caux, E., & Caselli, P. (2014). Herschel finds evidence for stellar wind particles in a protostellar envelope: is this what happened to the young sun?. *The Astrophysical journal letters*, *790*(1), L1.

[18] Jørgensen, J. K., Belloche, A., & Garrod, R. T. (2020). Astrochemistry during the formation of stars. *Annual Review of Astronomy and Astrophysics*, *58*(1), 727-778.

[19] Bethe, H. A. (1939). Energy production in stars. *Physical Review*, *55*(5), 434.

[20] von Weizsäcker, C. F. F. (1938). *Über Elementumwandlungen im Inneren der Sterne. II*. S. Hirzel.

[21] Arcones, A., & Thielemann, F. K. (2013). Neutrino-driven wind simulations and nucleosynthesis of heavy elements. *Journal of Physics G: Nuclear and Particle Physics*, *40*(1), 013201.

[22] Adelberger, E. G., García, A., Robertson, R. H., Snover, K. A., Balantekin, A. B., Heeger, K., ... & Typel, S. (2011). Solar fusion cross sections. II. The pp chain and CNO cycles. *Reviews of Modern Physics*, *83*(1), 195-245.

[23] Bahcall, J. N. (1989). *Neutrino astrophysics*. Cambridge University Press.

[24] Borexino Collaboration. (2018). Comprehensive measurement of pp-chain solar neutrinos. *Nature,* 562(7728), 505–510.

[25] Klessen, R. S., & Glover, S. C. (2023). The first stars: formation, properties and impact. *Annual*

Review of Astronomy and Astrophysics, *61*(1), 65-130.

[26] Maeder, A. (2008). *Physics, formation and evolution of rotating stars*. Springer Science & Business Media.

[27] Przybilla, N., Nieva, M. F., & Butler, K. (2008). A cosmic abundance standard: chemical homogeneity of the solar neighborhood and the ISM dust-phase composition. *The Astrophysical Journal Letters*, *688*(2), L103-L106.

[28] Langer, N., & Kudritzki, R. P. (2014). The spectroscopic hertzsprung-russell diagram. *Astronomy & Astrophysics*, *564*, A52.

[29] Salpeter, E. E. (1952). Nuclear reactions in stars without hydrogen. *Astrophysical Journal, vol. 115, p. 326-328*, *115*, 326-328.

[30] Hoyle, F. (1954). On Nuclear Reactions Occuring in Very Hot STARS. I. the Synthesis of Elements from Carbon to Nickel. *Astrophysical Journal Supplement, vol. 1, p. 121 (1954)*, *1*, 121.

[31] Drout, M. R., Piro, A. L., Shappee, B. J., Kilpatrick, C. D., Simon, J. D., Contreras, C., ... & Whitten, D. D. (2017). Light curves of the neutron star merger GW170817/SSS17a: Implications for r-process nucleosynthesis. *Science*, *358*(6370), 1570-1574.

[32] Kobayashi, C., Karakas, A. I., & Lugaro, M. (2020). The origin of elements from carbon to uranium. *The Astrophysical Journal*, *900*(2), 179.

[33] Deboer, R. J., Görres, J., Wiescher, M., Azuma, R. E., Best, A., Brune, C. R., ... & Uberseder, E. (2017). The C 12 (α, γ) O 16 reaction and its implications for stellar helium burning. *Reviews of Modern Physics*, *89*(3), 035007.

[34] Woosley, S. E., Heger, A., & Weaver, T. A. (2002). The evolution and explosion of massive stars. *Reviews of modern physics*, *74*(4), 1015.

[35] Busso, M., Gallino, R., & Wasserburg, G. J. (1999). Nucleosynthesis in asymptotic giant branch stars: Relevance for galactic enrichment and solar system formation. *Annual Review of Astronomy and Astrophysics*, *37*(1), 239-309.

[36] Arnett, W. D. (1982). Type I supernovae. I-Analytic solutions for the early part of the light curve. *Astrophysical Journal, Part 1, vol. 253, Feb. 15, 1982, p. 785-797.*, *253*, 785-797.

[37] Hix, W. R., & Thielemann, F. K. (1999). Silicon burning. II. Quasi-equilibrium and explosive burning. *The Astrophysical Journal*, *511*(2), 862-875.

[38] Mumpower, M. R., Surman, R., McLaughlin, G. C., & Aprahamian, A. (2016). The impact of individual nuclear properties on r-process nucleosynthesis. *Progress in Particle and Nuclear Physics*, *86*, 86-126.

[39] Käppeler, F., Gallino, R., Bisterzo, S., & Aoki, W. (2011). The s process: Nuclear physics, stellar models and observations. *Reviews of Modern Physics*, *83*(1), 157-193.

[40] Cowan, J. J., Sneden, C., Lawler, J. E., Aprahamian, A., Wiescher, M., Langanke, K., .& Thielemann, F. K. (2021). Origin of the heaviest elements: The rapid neutron-capture process. *Reviews of Modern Physics*, *93*(1), 015002.

[41] Thielemann, F. K., Eichler, M., Panov, I. V., & Wehmeyer, B. (2017). Neutron star mergers and nucleosynthesis of heavy elements. *Annual Review of Nuclear and Particle Science*, *67*, 253-274.

[42] Abbott, B. P., Abbott, R., Abbott, T. D., Acernese, F., Ackley, K., Adams, C., ... & Cahillane, C. (2017). GW170817: observation of gravitational waves from a binary neutron star inspiral. *Physical review letters*, *119*(16), 161101.

[43] Pian, E., D'Avanzo, P., Benetti, S., Branchesi, M., Brocato, E., Campana, S., ... & Vergani, D. (2017). Spectroscopic identification of r-process nucleosynthesis in a double neutron-star merger. *Nature*, *551*(7678), 67-70.

[44] Siegel, D. M., Barnes, J., & Metzger, B. D. (2019). Collapsars as a major source of r-process elements. *Nature*, *569*(7755), 241-244.

[45] Arnould, M., & Goriely, S. (2003). The p-process of stellar nucleosynthesis: astrophysics and nuclear physics status. *Physics Reports*, *384*(1-2), 1-84.

[46] Johnson, J. A. (2019). Populating the periodic table: Nucleosynthesis of the elements. *Science*, *363*(6426), 474-478.

[47] Herwig, F. (2005). Evolution of asymptotic giant branch stars. *Annu. Rev. Astron. Astrophys.*, *43*(1), 435-479.

[48] Sukhbold, T., Ertl, T., Woosley, S. E., Brown, J. M., & Janka, H. T. (2016). Core-collapse

supernovae from 9 to 120 solar masses based on neutrino-powered explosions. *The Astrophysical Journal*, *821*(1), 38.

[49] Janka, H. T. (2012). Explosion mechanisms of core-collapse supernovae. *Annual Review of Nuclear and Particle Science*, *62*(1), 407-451.

[50] Hillebrandt, W., & Niemeyer, J. C. (2000). Type Ia supernova explosion models. *Annual Review of Astronomy and Astrophysics*, *38*(1), 191-230.

[51] Maoz, D., Mannucci, F., & Nelemans, G. (2014). Observational clues to the progenitors of Type Ia supernovae. Annual Review of Astronomy and Astrophysics, 52, 107–170.

[52] Watson, D., Hansen, C. J., Selsing, J., Koch, A., Malesani, D. B. andersen, A. C., ... & Pian, E. (2019). Identification of strontium in the merger of two neutron stars. *Nature*, *574*(7779), 497-500.

[53] Kasen, D., Metzger, B., Barnes, J., Quataert, E., & Ramirez-Ruiz, E. (2017). Origin of the heavy elements in binary neutron-star mergers from a gravitational-wave event. *Nature*, *551*(7678), 80-84.

[54] Metzger, B. D. (2020). Kilonovae. *Living Reviews in Relativity*, *23*(1), 1.

[55] Matteucci, F. (2012). *Chemical evolution of galaxies*. Springer Science & Business Media.

[56] Scholberg, K. (2012). Supernova neutrino detection. *Annual Review of Nuclear and Particle Science*, *62*(1), 81-103.

[57] Tinsley, B. M. (1979). Stellar lifetimes and abundance ratios in chemical evolution. *Astrophysical Journal, Part 1, vol. 229, May 1, 1979, p. 1046-1056. Research supported by the Alfred P. Sloan Foundation*, *229*, 1046-1056.

[58] Frebel, A., & Norris, J. E. (2015). Near-field cosmology with extremely metal-poor stars. *Annual Review of Astronomy and Astrophysics*, *53*(1), 631-688.

[59] Beers, T. C., & Christlieb, N. (2005). The discovery and analysis of very metal-poor stars in the galaxy. *Annu. Rev. Astron. Astrophys.*, *43*(1), 531-580.

[60] Buder, S., Sharma, S., Kos, J., Amarsi, A. M., Nordlander, T., Lind, K., ...& Galah Collaboration. (2021). The GALAH+ survey: Third data release. *Monthly Notices of the Royal Astronomical Society*, *506*(1), 150-201.

[61] Weinberg, D. H., Holtzman, J. A., Hasselquist, S., Bird, J. C., Johnson, J. A., Shetrone, M., ... & Zamora, O. (2019). Chemical cartography with APOGEE: multi-element abundance ratios. *The Astrophysical Journal*, *874*(1), 102.

[62] Ji, A. P., Frebel, A., Chiti, A., & Simon, J. D. (2016). R-process enrichment from a single event in an ancient dwarf galaxy. *Nature*, *531*(7596), 610-613.

[63] Mösta, P., Roberts, L. F., Halevi, G., Ott, C. D., Lippuner, J., Haas, R., & Schnetter, E. (2018). r-process Nucleosynthesis from Three-dimensional Magnetorotational Core-collapse Supernovae. *The Astrophysical Journal*, *864*(2), 171.